Autoregulation of regulatory proteins is key for dynamic operation of *GAL* switch in *Saccharomyces cerevisiae*

Anurag Ruhela[a], Malkhey Verma[a], Jeremy S. Edwards[c], P.J. Bhat[b], Sharad Bhartiya[a,*], K.V. Venkatesh[a,b,*]

[a] *Department of Chemical Engineering, Indian Institute of Technology Bombay, Powai, Mumbai 400 076, India*
[b] *School of Bioscience and Bioengineering, Indian Institute of Technology Bombay, Powai, Mumbai 400 076, India*
[c] *Department of Chemical Engineering, University of Delaware, Newark, DE 19711, USA*

Received 5 July 2004; revised 30 August 2004; accepted 2 September 2004

Available online 15 September 2004

Edited by Takashi Gojobori

Abstract Autoregulation and nucleocytoplasmic shuttling play important roles in the operation of the *GAL* regulatory system. However, the significance of these mechanisms in the overall operation of the switch is unclear. In this work, we develop a dynamic model for the *GAL* system and further validate the same using steady-state and dynamic experimental expression data. Next, the model is used to delineate the relevance of shuttling and autoregulation in response to inducing, repressing, and non-inducing–non-repressing media. The analysis indicates that autoregulation of the repressor, Gal80p, is key in obtaining three distinct steady states in response to the three media. In particular, the analysis rationalizes the intuitively paradoxical observation that the concentration of repressor, Gal80p, actually increases in response to an increase in the inducer concentration. On the other hand, although nucleocytoplasmic shuttling does not affect the dynamics of the system, it plays a dominant role in obtaining a sensitive response to galactose. The dynamic model was also used to obtain insights on the preculturing effect on the system behavior.

Keywords: Autoregulation; *GAL* switch; Dynamic model; Systems biology; Nucleo-cytoplasmic shuttling; *Saccharomyces cerevisiae*

1. Introduction

Multiple interactions between various components in cellular regulation result in a complex network. Network regulation is hierarchical in nature with controls residing at metabolite, protein, mRNA, and DNA levels. These controls are achieved via interactions, which have been characterized as allosteric, protein–protein, and protein–DNA [1]. The interactions play the role of signal transducing elements, which repress or activate a regulatory switch. However, there exist other elements of the regulatory network such as autoregulation [2,3], compartmentalization of protein [4] and stoichiometry (for example, dimerization) [1,5], whose role in the overall performance of the regulatory switch is unclear. In silico modeling of these networks, in addition to experimental investigations, assists in eliciting the role of these individual elements in the overall regulation. Indeed, a large number of steady state in silico models for different regulatory networks have been reported in the literature such as *lac* operon [6], bacteriophage λ [7], the *trp* repressor [8], and *GAL* system in yeast [9]. Development of steady-state models is relatively easy, since it only requires binding constants and the total inventory of the participating components. Binding constants quantify strength of interaction and may be obtained through in vitro experiments. Steady-state models can be used to evaluate the network sensitivity to its mechanistic elements. Thus, for example it has been demonstrated by using such a steady-state modeling approach that cooperativity is essential for ultrasensitive switching between lytic and lysogeny in lambdaphage [7]. A similar steady-state approach has been used to show that nucleocytoplasmic shuttling plays a vital role in obtaining a sensitive response to galactose in the *GAL* system of *Saccharomyces cerevisiae* [9].

Although the steady-state modeling approach provides insights into the in vivo operation of the network, it fails to capture the temporal relevance of the individual elements in the overall performance of the switch. This motivates the development of a dynamic modeling approach. In particular, dynamic models underscore the temporal dominance of one mechanism over the other, whereas steady-state models only address questions regarding the final relative roles of each mechanism. For example, Venkatesh et al. [10] used a dynamic model to illustrate the robust performance of the *trp* system due to the existence of multiple feedback loops. However, development of dynamic models necessitates additional experimental data to quantify kinetic rate constants for transcription and translation. In this work, we present a dynamic model of the *GAL* regulatory network of *S. cerevisiae*, which represents a well-characterized eukaryotic switch. Further, the dynamic model is used to identify the relevance of autoregulation of regulatory proteins Gal3p and Gal80p as well as the nucleocytoplasmic shuttling of Gal80p. Our analysis demonstrates that autoregulation is key for the switch to reside in three states, namely, repressed in the presence of glucose, activated in the presence of galactose, and incompletely repressed in a non-inducing–non-repressing (NINR) medium.

* Corresponding authors. Fax: +91-22-25726895.
E-mail addresses: bhartiya@che.iitb.ac.in (S. Bhartiya), venks@che.iitb.ac.in (K.V. Venkatesh).

0014-5793/$22.00
doi:10.1016/j.febslet.2004.09.001

2. The GAL regulatory network

The *GAL* gene family is a set of structural and regulatory genes that enable cells to utilize galactose as a carbon source [1]. The *GAL* regulatory network comprises of a transcriptional activator protein Gal4p, a repressor protein Gal80p, and a signal transducer protein Gal3p [1,5,11–14]. In a NINR medium such as glycerol, Gal80p binds to the activation domain of Gal4p bound to the DNA, thereby inhibiting the expression of *GAL* genes [1,5]. However, in the presence of galactose, Gal3p is activated to form a complex with Gal80p in the cytoplasm. This leads to shuttling of Gal80p from the nucleus to the cytoplasm, thereby greatly reducing the availability of Gal80p for binding to Gal4p in the nucleus [15]. Thus, galactose relieves repression through nucleocytoplasmic shuttling of Gal80p. In the presence of glucose, synthesis of Gal4p is inhibited through an independent Mig1p mediated repression of *GAL* genes [16–18]. It should be noted that the regulatory proteins, Gal80p and Gal3p, are themselves regulated by the expression of the *GAL* regulatory switch [9].

Nucleocytoplasmic shuttling and autoregulation play an important role in the operation of the *GAL* regulatory switch in addition to protein–DNA and protein–protein interactions (including dimerization). Using a steady-state model, Verma et al. [9] have demonstrated that the nucleocytoplasmic shuttling of Gal80p is responsible for the sensitive response of *GAL* switch to galactose. However, their steady-state model predicted a similar response in both the presence and absence of autoregulation, and therefore could not delineate the relevance of autoregulation. Thus, one may question the role of autoregulation of the repressor, Gal80p, and the activator, Gal3p, in the dynamic performance of the system. The dynamic model presented here also addresses the effect of preculturing state (either on glucose or NINR) on the expression of *GAL* genes.

3. Methods

A schematic of the *GAL* regulatory network in *S. cerevisiae* is shown in Fig. 1. The model accounts for transcriptional interaction of dimer Gal4p with three genes having one binding site, namely *GAL3*, *GAL80*, and *MEL1* [1] identified as D1, and with seven genes having two binding sites, namely *GAL1*, *GAL2*, *GAL7*, *GAL10*, *MTH1*, *PCL10*, and *FUR10* [1,19] identified as D2. The fractional transcriptional levels for D1 and D2 are described by

$$f_1 = \frac{[\text{D1-Gal4p}_2]}{[\text{D1}_t]} \tag{1}$$

$$f_2 = \frac{[\text{D2-Gal4p}_2] + [\text{D2-Gal4p}_2\text{-Gal4p}_2]}{[\text{D2}_t]} \tag{2}$$

[D1-Gal4p$_2$] represents interaction of dimer Gal4p with DNA for genes with one binding site, while [D1$_t$] is the total operator concentration of genes with one binding site for Gal4p. It can be noted that expression for genes with two binding sites occurs when either of the two binding sites are bound by Gal4p, that is, [D2-Gal4p$_2$] or [D2-Gal4p$_2$-Gal4p$_2$]. The total available operator concentration of genes with two binding sites for Gal4p is [D2$_t$]. [D1]$_t$ and [D2]$_t$ were estimated as $3 \times 2.372 \times 10^{-11}$ and $7 \times 2.372 \times 10^{-11}$ M, respectively, assuming a total volume of 70 μm^3 for a yeast cell, where 2.372×10^{-11} M denotes concentration of one gene [22]. The development of the dynamic model is based on unsteady molar balances written for all the species in the network (see Fig. 1) and is detailed in Appendix A. The translation of structural protein by genes with one and two binding sites (P_1 and P_2, respectively) can be described by

$$\frac{dP_1}{dt} = k_{01} f_{1p} - \mu P_1 \tag{3}$$

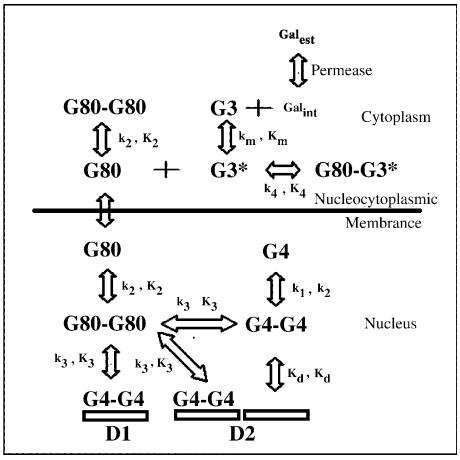

Fig. 1. Schematic of the interactions in wild-type strain. D1 and D2 represent genes with one and two binding sites, respectively. G4, G80, G3, and G3* represent regulatory proteins Gal4p, Gal80p, Gal3p, and activated Gal3p, respectively. Gal$_{ext}$ and Gal$_{int}$ represent the extraneous and intracellular galactose. K_i and k_i represent appropriate equilibrium dissociation constant and the forward kinetic rate constant, respectively.

$$\frac{dP_2}{dt} = k_{02} f_{2p} - \mu P_2 \tag{4}$$

P_1 represents protein expression of genes having only one binding site for Gal4p (such as *MEL1*), whereas P_2 represents protein expression of genes with two binding sites (such as *GAL1*). The fractional translation, quantified by f_{1p} and f_{2p}, is related to the fractional transcription in a non-linear fashion as follows:

$$f_{1p} = f_1^{0.5} \tag{5}$$

$$f_{2p} = f_2^{0.5} \tag{6}$$

The above equation captures the inefficiencies of the translation process, as all the mRNA that is transcribed is not converted to protein [20,21].

Synthesis of Gal4p is repressed by glucose and is modeled by a Michaelis–Menten type relationship

$$\text{Rate of Gal4p synthesis} = k_g[\text{Gal4p}_{max}]\left(\frac{K_i}{K_i + \text{Glu}_{ext}}\right) \tag{7}$$

where K_i and k_g represent the half-saturation constant and kinetic rate constant, respectively. The other two regulatory proteins, Gal3p and Gal80p, are autoregulated [9] by genes with one binding site. Thus, their synthesis is modeled as follows:

$$\text{Rate of Gal3p synthesis} = k_3 f_{1p} \text{D1}_t \tag{8}$$

$$\text{Rate of Gal80p synthesis} = k_{80} f_{1p} \text{D1}_t \tag{9}$$

where k_3 and k_{80} represent the respective translational kinetic constants.

The model accounts for the transport of extracellular galactose (Gal$_{ext}$) through the cytoplasmic membrane, which is controlled by permease (that is, Gal2p). Thus, the intracellular level of galactose (Gal$_{int}$) is determined as follows:

$$\frac{d[\text{Gal}_{int}]}{dt} = k_p[\text{Gal2p}]\frac{\text{Gal}_{ext}}{k_i + \text{Gal}_{ext}} - \mu \text{Gal}_{int} \tag{10}$$

where Gal2p is regulated by genes with two binding sites as follows:

$$\frac{d[\text{Gal2p}]}{dt} = k_e f_{2p} - \mu[\text{Gal2p}] \tag{11}$$

The activation of Gal3p by intracellular galactose is modeled by modifying the forward kinetic rate constant k_m as a function of the intracellular galactose concentration as shown

$$k_m = k_{max}\left(\frac{\text{Gal}_{int}}{K_s + \text{Gal}_{int}}\right) \tag{12}$$

Finally, the activated Gal3p binds to Gal80p inside the cytoplasm and prevents the shuttling of cytoplasmic Gal80p back into the nucleus.

A large number of parameters play a role in the response of the *GAL* system. Numerical values for equilibrium parameters (such as binding and shuttling constants), total component concentrations (such as total operator concentration, total concentration of proteins Gal3p, Gal80p, and Gal4p), and the specific growth rates have been reported in the literature [9,22]. Further, parameters quantifying activation of Gal3p by galactose and repression of Gal4p by glucose have also been identified in the literature [9]. All of the parameters referred to in the above affect the steady-state expression levels. The remaining parameter values needed to simulate the current model are the forward kinetic rate constants and their values dictate the dynamic aspects of the network performance. Seven such kinetic rate constants were used in the model presented in Appendix A. The values of these seven rate constants were selected by fitting the model predictions with the steady-state and dynamic data obtained through our experiments. Note that the backward kinetic rate constants were fixed by the equilibrium binding constants obtained from the literature [9]. The complete model consists of 23 ordinary differential equations. These along with the parameter values presented in Appendix A were solved using MATLAB's solver, 'ode15s' (The MathWorks Inc., USA).

4. Experimental protocol

4.1. Yeast strain

Saccharomyces cerevisiae strain Sc 753 [23] with genotype *GAL4::GAL80::gal1* was used to measure the dynamic expression of α-galactosidase from *MEL1*, a structural *GAL* gene having one binding site for Gal4p. This strain is unable to utilize galactose due to the absence of *GAL1* gene. Therefore, the inducer (galactose) is not metabolized but merely triggers induction.

4.2. Medium for the preculture and innoculum size

A cotton-stoppered, 500 ml Erlenmeyer flask containing 100 ml medium of the following composition: 25 mg/L adenine, 5.0 g/L Yeast extract, 10.0 g/L peptone, and 30.0 g/L glycerol was used. The pH was adjusted to 5.5 with 1 M HCl. The cells were grown in shake flask at 240 rpm on a rotary shaker at 30 °C for 12–16 h, till the cell concentration had reached 1.0–1.5 OD at 600 nm. Subsequently, the bioreactor was inoculated with 10% cell mass of OD one at 600 nm.

4.3. Cultivation conditions

Strain Sc 753 was grown in the same media as the preculturing medium in a batch bioreactor until biomass reached an OD of 0.5–0.75 at 600 nm after which the standard galactose solution was added by a calibrated peristaltic pump to provide a predetermined steady-state galactose concentration, which was maintained during the course of the batch. The bioreactor (Vaspan Industries, Mumbai, India) was a 2 L (1 L working volume) stirred tank reactor, with two Rushton turbines. The dissolved oxygen and pH data were obtained online using probes (Bela Insruments, Mumbai, India) interfaced with a PC, at an airflow rate of 1.5 Lpm and 300 rpm agitation. A separate experiment was performed by adding a standard glucose solution, the details of which have been provided by Verma et al. [22].

4.4. Analyses

The samples were taken aseptically at different time points after the addition of galactose. The α-galactosidase activity was measured in the fermented broth by the method described by Post-Beittenmiller et al. [24]. In the fermented broth, galactose was separated by Biorad Aminex HPX-87H column and concentration was measured refractometrically using La-Chrom L-7490 RI detector (Merck, Germany). All the experiments were repeated on different days and the deviation in data was within acceptable limits with a maximum variation of 9.0%. The steady-state data of repression by glucose on the expression of α-galactosidase (from gene having one binding site for Gal4p) and β-galactosidase (from gene having two binding sites for Gal4p) for a mutant strain lacking Gal80p have been taken from Verma et al. [22].

5. Results

The dynamic model was validated using experimental data. Fig. 2A shows the fractional protein expression at steady state for a strain lacking Gal80p for varying glucose concentrations. Absence of Gal80p in the mutant strain eliminates all interactions of Gal80p with Gal4p as well as Gal3p. Thus, the *GAL* regulatory network responds to changes in Gal4p concentra-

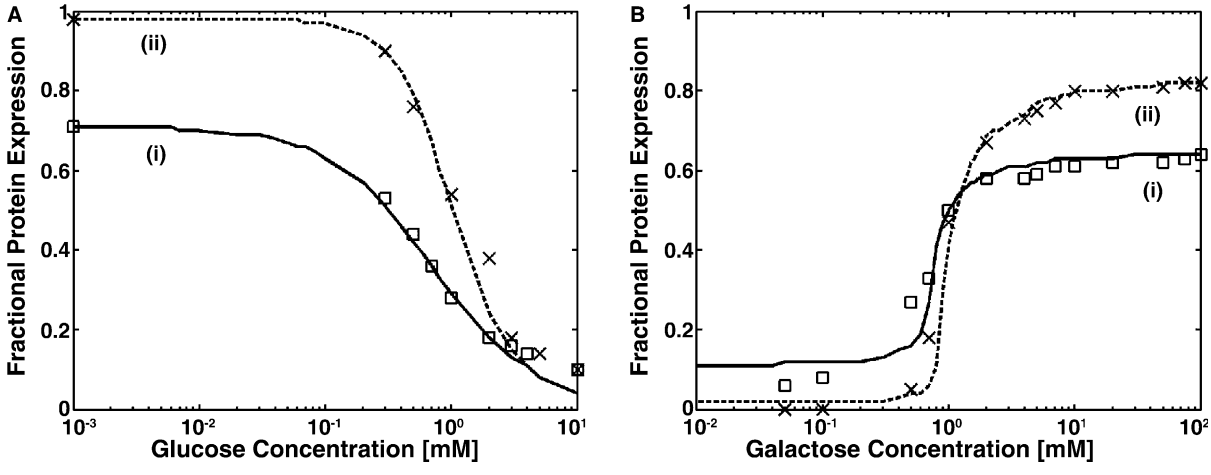

Fig. 2. (A) Variation in protein expression at steady state with change in glucose concentration for mutant strain. (B) Model predictions compared to the experimental data as a function of galactose levels for wild-type strain. (i) The plot of expression of genes with one binding site; (ii) the plot of expression of genes with two binding sites.

tion alone, which is repressed by glucose. It is observed that the switch is completely shut off at about 9.5 mM glucose, with the maximum expression for genes with one and two binding sites being 72% and 98%, respectively. A similar comparison of the steady-state fractional protein expression for the strain Sc 753 lacking *GAL1* at different levels of galactose is depicted in Fig. 2B. The maximum expressions for genes with one and two binding sites are noted as 64% and 82%, respectively, and occur at galactose levels of 5 mM. It is observed that the expression for genes with two binding sites is more sensitive than genes with one binding site for changes in galactose level.

Comparing Fig. 2A and B, it is clear that the expression levels of the strain lacking *GAL80* are higher than those in the strain lacking *GAL1*. This implies that there is incomplete sequestration of Gal80p in the wild-type strain even in the presence of high galactose concentrations. On the other hand, in the absence of galactose, genes with one binding sites are not completely shut off and show "leaky transcription" of about 5–10%, whereas the genes with two binding sites are completely repressed. The agreement between the model predictions and the experimental steady-state protein expressions in Fig. 2A and B validates the developed model.

Subsequent results presented here refer to expression from *MEL1*, which is a *GAL* gene with one binding site for Gal4p. Fig. 3A shows the comparison between model predictions and experimentally obtained dynamic protein expression levels of the strain Sc 753 precultured on glycerol (NINR) at two different galactose concentrations, namely 15 mM (curve (i)) and 5 mM (curve (ii)). It is noted that curve (ii) has been normalized by two to ensure clarity. At time $t = 0$, the expression level is about 10%, which is observed in a NINR medium. Upon exposing the cells to a galactose concentration of 15 mM (curve (i)), the genes fully express themselves in about $t = 25$ h. When exposed to 5 mM galactose medium (curve (ii)), the network responds similar to that when exposed to 15 mM galactose medium (the difference between the two as observed in the figure is due to scaling). Fig. 3B also depicts the dynamic variation of fractional protein expression for the strain Sc 753 when precultured on glucose, when exposed to two different galactose concentrations namely, 15 mM (curve (i)) and 5 mM (curve (ii)). As glucose represses Gal4p, the regulatory network is completely shut off at $t = 0$. Further, it is noted that the protein expression levels reach their steady-state values faster than in the case where the cells are precultured on NINR me-

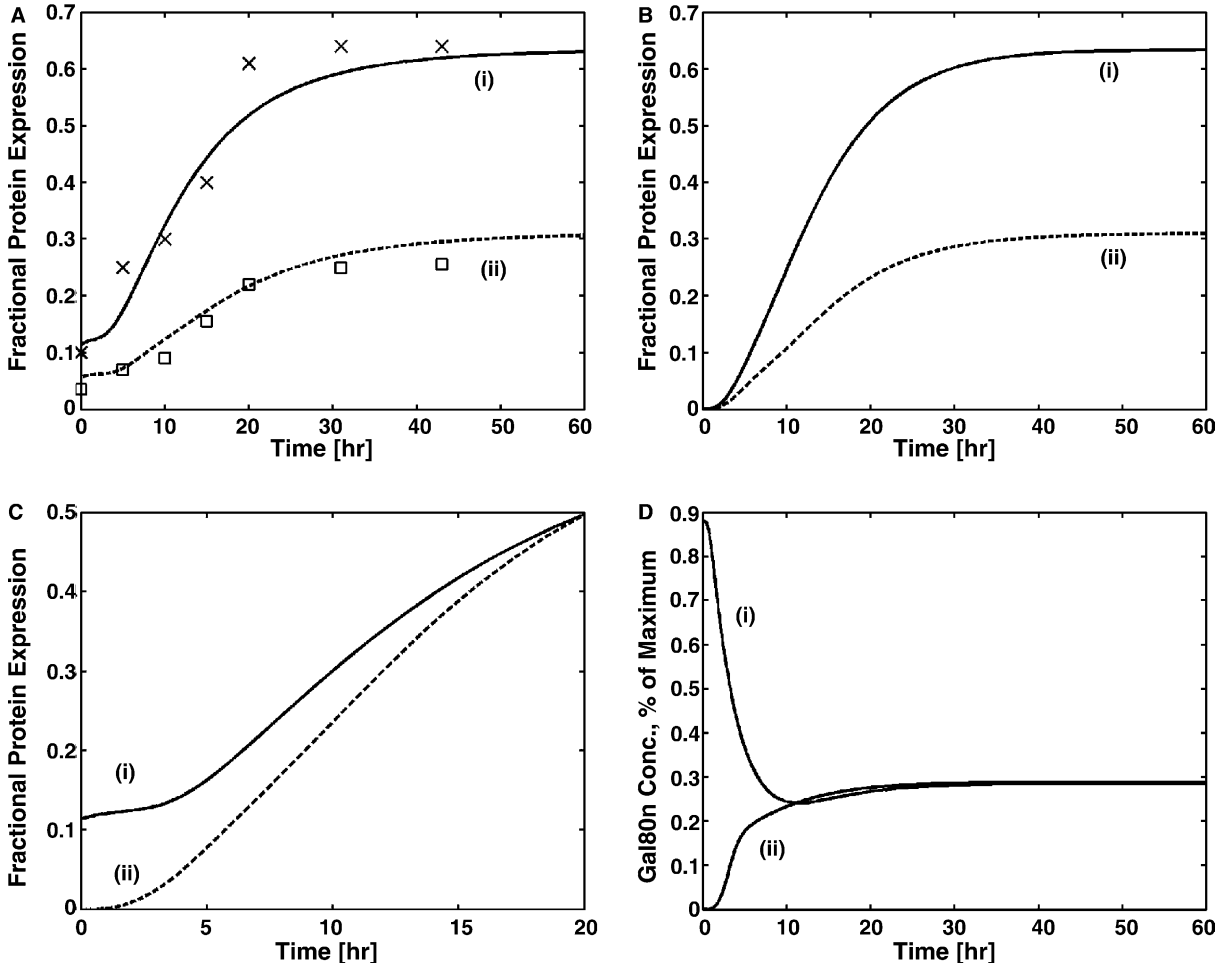

Fig. 3. (A) Variation of fractional protein expression for genes with one binding site with time for extraneous galactose level = 15 mM (i) and 5 mM (ii), compared with the experimental data. Curve (ii) is normalized by 2 for clarity (precultured in NINR medium). (B) Variation of fractional protein expression for genes with one binding site with time for different extraneous galactose levels. (i) Plot with galactose = 15 mM; (ii) plot with galactose = 5 mM (normalized by 2). (C) Difference in "lag" due to the difference in preculturing environments. (i) The case when system is precultured in NINR medium; (ii) the case with glucose preculturing. (D) Percentage concentration of Gal80p inside nucleus normalized with respect to 0.64 μM at galactose concentration = 100 mM. (i) The case with NINR preculturing; (ii) the case with glucose preculturing.

dium (compare Fig. 3A with B). Fig. 3C shows the difference in the initial lag of transcription in the presence of 15 mM of galactose in the medium when the system is precultured on glycerol (curve (i)) and when it is precultured on glucose (curve (ii)). It is observed that there is a distinct initial "dead phase" when precultured on glycerol. The effect of preculturing medium has been further clarified in Fig. 3D, which depicts the concentration of Gal80p inside the nucleus alone. Curve (i) shows the dynamic concentration of Gal80p in the nucleus when cells were precultured in NINR medium and exposed to a 15 mM galactose medium at $t = 0$. The activation of Gal3p by galactose causes sequestration of the Gal80p in the cytoplasm causing shuttling of Gal80p from the nucleus to the cytoplasm. This leads to a decrease in the Gal80p concentration in the nucleus as depicted in curve (i) where the nuclear Gal80p concentration reduces from about 1% (0.11 μM) to 0.25% (0.02 μM). This also implies that a mere 1% of Gal80p in the nucleus is sufficient to repress up to 10% protein expression as observed in an NINR medium. Further, irrespective of the preculturing condition, the concentration of the complex Ga80p–Gal3p in the cytoplasm increases from 0 to 0.58 μM on addition of galactose. Hence, although the addition of galactose increases the concentration of repressor Gal80p, through autoregulation, 91% of Gal80p exists as Ga80p–Gal3p complex in the cytoplasm. However, when precultured in glucose medium, Gal80p is completely absent in the nucleus until $t = 0$. At $t = 0$, it is exposed to 15 mM galactose medium. At this instant, the synthesis of Gal4p and the corresponding increased protein expressions lead to synthesis of Gal80p in the cytoplasm, some of which translocates to the nucleus thus showing a slight increase in the nuclear Gal80p levels as depicted by curve (ii) in Fig. 3D. Although preculturing has a very significant impact on the initial dynamics of Gal80p, the steady-state concentrations are unaffected as observed by the convergence of curves (i) and (ii) after $t = 25$ h. This indicates that the dead phase observed when precultured on NINR medium is due to shuttling of Gal80p from the nucleus but does not affect the final steady-state protein expression.

It is of interest to identify the role of autoregulation of regulatory proteins Gal3p and Gal80p in the dynamic operation of the switch. Experiments and steady-state theoretical analysis of the *GAL* regulatory network fail to provide insights into the significance of autoregulation of regulatory proteins [9]. We make use of the dynamic model to study this issue by appro-

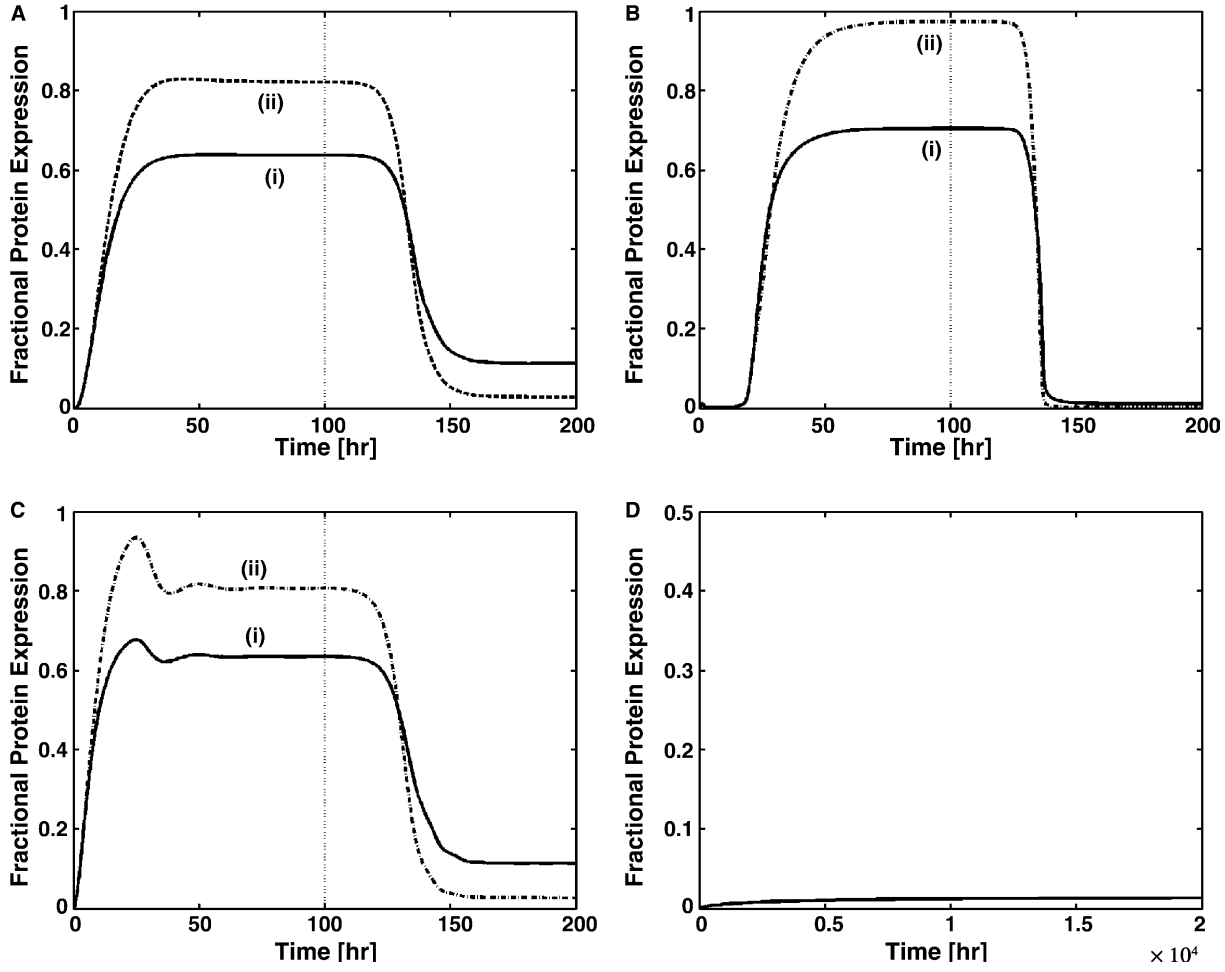

Fig. 4. (A) Switch performance evaluated under a step change to extraneous galactose levels. (B) Switch performance evaluated under a step change to extraneous galactose levels when both regulatory proteins are independently expressed. (C) Switch performance evaluated under a step change to extraneous galactose levels when Gal3p is independently expressed. (D) Switch performance evaluated under a step change to extraneous galactose levels when Gal80p is independently expressed. (i) The plot of expression of genes with one binding site; (ii) the plot of expression of genes with two binding sites. In each of the above, the extraneous galactose was changed from 0 to 15 mM at time $t = 0$. Subsequently, at $t = 100$ h the extraneous galactose was changed from 15 to 0 mM.

priately modifying the model equations that reflect autoregulation. Fig. 4A shows the expression profile for genes with one binding site (curve (i)) and genes with two binding sites (curve (ii)) when the wild-type cells are precultured on glucose. In this case, the cells express fully in about 25 h when exposed to a galactose-rich medium at $t = 0$ h. When the environment is depleted of galactose at $t = 100$ h, the protein expressions attain a new steady state, which matches with the steady state attained in NINR medium. The dead phase observed at $t = 100$ h is on account of shuttling of Gal80p from the cytoplasm into the nucleus. Fig. 4B shows the performance of the network in the absence of autoregulation of both the Gal3p and Gal80p. In this case, addition of galactose at $t = 0$ is followed by a long dead phase of 15 h before the network expression commences. The long dead phase represents the time needed for removal of excess and unregulated Gal80p from the nucleus. Further, on removal of galactose at $t = 100$ h, the network completely shuts off and does not exhibit the leaky behavior as seen in wild type due to excess of unregulated Gal80p in the nucleus. Absence of autoregulation of Gal3p alone is shown in Fig. 4C. With the exception of the overshoot observed at $t = 15$ h, the switch shows similar behavior as the wild type. Fig. 4D shows the protein expression in the absence of autoregulation of Gal80p alone, that is, Gal3p is autoregulated. In this case, Gal3p concentration is always limited by its autoregulation and therefore fails to sequester the large excess of Gal80p from the nucleus. This results in the failure of the network to respond to galactose. The above analysis of autoregulation moots the conclusion that autoregulation of Gal80p is essential for the operation of the network.

6. Discussion

The *GAL* network represents a complex inter-play between various mechanisms and regulatory proteins. Specifically, shuttling of Gal80p and autoregulation of regulatory proteins constitute two mechanisms that play a pivotal role in the operation of the switch. At this stage, it is relevant to question the significance of these two mechanisms. It is intuitively paradoxical that concentration of a repressor protein, Gal80p, increases with the inducer concentration (galactose) through autoregulation. Further, Gal3p is also autoregulated in response to the inducer. How do these regulatory proteins influence the dynamic operation of the switch through autoregulation? We have used a dynamic model of the switch to analyze the roles of individual proteins in the overall operation.

The *GAL* system resides in three steady states: (i) completely repressed by glucose; (ii) weakly repressed in NINR medium (lactate or glycerol); and (iii) induced by galactose. In the presence of glucose, due to reduced Gal4p concentration the DNA binding sites are essentially free. In an NINR medium, Gal80p is bound to DNA–Gal4p complex in the nucleus to yield a leaky response (see Fig. 2B). Further, in the presence of galactose, the Gal80p is sequestered from the nucleus by cytoplasmic Gal3p to express the *GAL* genes [9,15].

In the absence of autoregulation of both the regulatory proteins (see Fig. 4B), the response of the switch in an NINR medium is similar to that in glucose. Thus, the three unique responses observed in the wild-type degenerate to two. When autoregulation of Gal80p alone is restored, the leaky character of the protein expression reappears (see Fig. 4C). On the other hand, when autoregulation of Gal3p alone is considered, the large amounts of unregulated Gal80p continue to repress protein expression even in the presence of galactose. The above analysis reveals that the autoregulation of Gal80p is essential for the *GAL* switch to reside in three unique phenotypical states. A similar analysis for Gal3p demonstrates that autoregulation of Gal3p is not essential for obtaining the three unique physiological states of the *GAL* switch. However, autoregulation of Gal3p appears to dampen the speed of protein expression when exposed to galactose. Further, it is known that Gal3p has evolved from Gal1p through duplication in order to delink the metabolic process (Gal1p) from the genetic switch (Gal3p) [25]. It has also been shown that the promoter of Gal1p has been retained in Gal3p leading to its autoregulation.

Other than autoregulation, nucleocytoplasmic shuttling of Gal80p has been demonstrated to play a vital role in the performance of the switch [9,15]. The variations in the distribution coefficient for shuttling by maintaining the same forward kinetic rate constants do not influence the dynamic behavior of protein expression (results not shown). However, it has a dramatic effect on the steady-state values of protein expression. The value of the distribution coefficient decides the degree of sensitivity (steepness) of the steady-state response to galactose concentration [9]. Thus, the response of the *GAL* switch to galactose is mainly influenced by autoregulation and shuttling.

Unlike the case where the cells are exposed to galactose, the response of the *GAL* system to glucose is merely dependent on the Gal4p concentration, since Gal4p is repressed by glucose. In this case, the dominant mechanism in the operation of the *GAL* switch is the interaction of Gal4p with multiple binding sites (UAS). As seen in Fig. 2A, repression of genes with two binding sites is more sensitive than those with one binding site to glucose concentration. Gal4p prefers binding to genes with two sites due to the presence of cooperativity, which represents another mechanism that affects the operation of the switch. This results in limiting Gal4p concentration available for binding to genes with one binding site. Consequently, genes with one binding site are expressed to about 70% as seen in the mutant strain lacking Gal80p (see Fig. 2A). In case of NINR medium, a leaky expression is observed due to limiting Gal80p concentration in the nucleus [5,9]. The main mechanistic cause for this incomplete expression is the autoregulation of Gal80p (see Fig. 4). A coordinated increase of both the Gal80p and Gal3p through the switch ensures two steady states, one leaky in the absence of galactose and the other completely expressed in the presence of galactose.

The dynamic model can be used to analyze the effect of preculturing on the *GAL* gene expression. When precultured on glucose, the initial protein expression is completely absent. In the presence of galactose, Gal4p is synthesized and binds to the DNA binding sites of the *GAL* gene to start transcription (see Fig. 3C). Further, Gal80p is also synthesized in the cytoplasm, but becomes immediately sequestered thereby eliminating the effect of shuttling. In case of preculturing on NINR medium, Gal80p is bound to the DNA–Gal4p complex resulting in a leaky expression even in the absence of galactose. In the presence of galactose, a lag phase of about 2 h is observed before transcription takes place (see Fig. 3C). Presumably this lag occurs due to Gal80p, which is already bound to Gal4p and further the bound Gal80p needs to be sequestered in order to begin transcription. On the other hand, when precultured on glucose, Gal80p is absent from the nucleus. This indicates that

the lag observed in case of preculturing in NINR medium is due to the rate limitation caused by Gal80p shuttling.

The molecular mechanisms of many regulatory switches have been elucidated through studies in molecular biology. In many instances, the relevance of the different mechanisms involved in the operation of the regulatory network is not clear. Dynamic models help in evaluating the inherent properties in the structure of a network that influences its operation. The complexity arising in the network may impart properties such as robustness, dynamic stability, and sensitive response to the switch [26,27]. Dynamic models can also answer questions regarding the relevance of a feedback interaction to the switch performance. For example, it has been recently demonstrated that multiple feedback loops in the *trp* operon lead to robust regulation in *Escherichia coli* [10]. A dynamic modeling approach as presented in this paper and its subsequent analysis can be used in obtaining design principles evolved in nature.

Appendix A

A.1. Model development

The first step in the development of the model was the identification of the various complexes present in the regulatory system. The complexes may be divided into two groups, viz. protein–protein complexes, and protein–DNA complexes. The next step involves listing the various interactions that take place amongst these complexes. This set of interactions had been adopted from Verma et al. [9]. The complete set is shown as a schematic in Fig. 1. In a steady-state model all the above interactions are assumed to be at steady-state and an equilibrium constant is associated with each of the those interactions.

In the development of dynamic model all the interactions shown in Fig. 1 are taken to be at unsteady state and corresponding dynamic molar balances were written for all the species in terms of kinetic and equilibrium constants. The complete dynamic model equations are presented below. For convenience the following notation is adopted:

$y_1 = [\text{Gal4p}]$
$y_2 = [\text{Gal4p}_2]$
$y_3 = [\text{D1}]$
$y_4 = [\text{D2}]$
$y_5 = [\text{D1-Gal4p}_2]$
$y_6 = [\text{D2-Gal4p}_2]$
$y_7 = [\text{D2-Gal4p}_2\text{-Gal4p}_2]$
$y_8 = [\text{Gal80pn}]$
$y_9 = [\text{Gal80pn}_2]$
$y_{10} = [\text{Gal4p}_2\text{-Gal80pn}_2]$
$y_{11} = [\text{D1-Gal4p}_2\text{-Gal80pn}_2]$
$y_{12} = [\text{D2-Gal4p}_2\text{-Gal80pn}_2]$
$y_{13} = [\text{D2-Gal4p}_2\text{-Gal80pn}_2\text{-Gal4p}_2]$
$y_{14} = [\text{D2-Gal4p}_2\text{Gal80pn}_2\text{-Gal4p}_2\text{-Gal80pn}_2]$
$y_{15} = [\text{Gal80pc}]$
$y_{16} = [\text{Gal80pc}_2]$
$y_{17} = [\text{Gal3p}]$
$y_{18} = [\text{Gal80pc-Gal3p*}]$
$y_{19} = [\text{Gal3p*}]$
$y_{20} = [\text{Gal2p}]$
$y_{21} = [\text{Gal}_{\text{int}}]$
$y_{22} = [\text{Mel1}]$

A.2. Ordinary differential equations

$$\frac{d[y_1]}{dt} = k_1K_1y_2 - k_1y_1^2 + K_g\left(\frac{K_i}{K_i + \text{Glu}_{\text{ext}}}\right) - \mu y_1 \tag{A.1}$$

$$\frac{d[y_2]}{dt} = \frac{k_1}{2}y_1^2 - k_1K_1y_2 + k_dK_dy_5 - k_dy_2y_3 + k_dK_dy_6 - k_dy_2y_4 + mk_dK_dy_7 - k_dy_2y_6 + k_3K_3y_{10} - k_3y_2y_9 - \mu y_2 \tag{A.2}$$

$$\frac{d[y_3]}{dt} = k_dK_dy_5 - k_dy_3y_2 \tag{A.3}$$

$$\frac{d[y_4]}{dt} = k_dK_dy_6 - k_dy_4y_2 \tag{A.4}$$

$$\frac{d[y_5]}{dt} = k_dy_2y_3 - k_dK_dy_5 + k_3K_3y_{11} - k_3y_9y_5 \tag{A.5}$$

$$\frac{d[y_6]}{dt} = k_dy_2y_4 - k_dK_dy_6 + k_dK_dy_7 - mk_dy_2y_6 + k_3K_3y_{12} - k_3y_9y_6 \tag{A.6}$$

$$\frac{d[y_7]}{dt} = mk_dy_2y_6 - k_dK_dy_7 + k_3K_3y_{13} - k_3y_9y_7 \tag{A.7}$$

$$\frac{d[y_8]}{dt} = k_2K_2y_9 - k_2y_8^2 + kKy_{15} - ky_8 - \mu y_8 \tag{A.8}$$

$$\frac{d[y_9]}{dt} = \frac{k_2}{2}y_8^2 - \frac{k_2}{2}K_2y_9 + k_3K_3y_{10} - k_3y_2y_9 + k_3K_3y_{11} - k_3y_9y_5 + k_3K_3y_{12} - k_3y_9y_6 + k_3K_3y_{13} - k_3y_9y_7 + k_3K_3y_{14} - k_3y_9y_{13} - \mu y_9 \tag{A.9}$$

$$\frac{d[y_{10}]}{dt} = k_3y_2y_9 - k_3K_3y_{10} - \mu y_{10} \tag{A.10}$$

$$\frac{d[y_{11}]}{dt} = k_3y_5y_9 - k_3K_3y_{11} \tag{A.11}$$

$$\frac{d[y_{12}]}{dt} = k_3y_6y_9 - k_3K_3y_{12} \tag{A.12}$$

$$\frac{d[y_{13}]}{dt} = k_3y_7y_9 - k_3K_3y_{13} + k_3K_3y_{14} - k_3y_{13}y_9 \tag{A.13}$$

$$\frac{d[y_{14}]}{dt} = k_3y_9y_{13} - k_3K_3y_{14} \tag{A.14}$$

$$\frac{d[y_{15}]}{dt} = k_2K_2y_{16} - k_2y_{15}^2 + ky_8 - kKy_{15} + k_4K_4y_{18} - k_4y_{15}y_{19} + K_{\text{t}}\text{D1}_{\text{t}}f_{1p} - \mu y_{15} \tag{A.15}$$

$$\frac{d[y_{16}]}{dt} = \frac{k_2}{2}y_{15}^2 - k_2K_2y_{16} - \mu y_{16} \tag{A.16}$$

$$\frac{d[y_{17}]}{dt} = k_{m1}y_{19} - k_my_{17} + K_{\text{t}}\text{D1}_{\text{t}}f_{1p} - \mu y_{17} \tag{A.17}$$

$$\frac{d[y_{18}]}{dt} = k_4y_{15}y_{19} - k_4K_4y_{18} - \mu y_{18} \tag{A.18}$$

$$\frac{d[y_{19}]}{dt} = k_4K_4y_{18} - k_4y_{15}y_{19} + k_my_{17} - k_{m1}y_{19} - \mu y_{19} \tag{A.19}$$

Table 1
Normalization constants

Variable	Normalization constant
Gal4p, Gal4p$_2$, Gal80pn$_2$-Gal4p$_2$	[Gal4p]$_t$
All D1-complexes	[D1]$_t$
All D2-complexes	[D2]$_t$
Gal80pc, Gal80pc$_2$, Gal80pn, Gal80pn$_2$, Gal2p	[Gal80p]$_{max}$
Gal3p, Gal3p*	[Gal3p]$_{max}$
Gal$_{int}$	[Gal$_{int}$]$_{max}$

Table 2
Model parameters

Parameter	Value	Parameter	Value
K_d	2×10^{-10} M	k_d	3.0×10^{-9} h^{-1}
K	0.4	k	1.25×10^{-2} h^{-1}
K_s	0.08 M	k_p	1.21×10^{3} h^{-1}
K_t	3×10^{3} h^{-1}	k_m	Depends on Gal$_{int}$
K_p	8.0×10^{3} h^{-1}	k_{m1}	1.0×10^{-3} h^{-1}
K_i	4×10^{-4} M	k_{max}	1.0×10^{3} h^{-1}
k_i	0.12 M	k_1	1.0×10^{7} h^{-1}
K_g	1.15×10^{-9} M h^{-1}	k_2	7.0×10^{6} h^{-1}
K_1	1.00×10^{-7} M	k_3	1.0×10^{13} h^{-1}
K_2	1.00×10^{-10} M	k_4	5.0×10^{8} h^{-1}
K_3	3.0×10^{-9} M	μ	0.2 h^{-1}
K_4	6.30×10^{-11} M	m	30
k_{me}	2.80×10^{-3} h^{-1}	D1$_t$	7.12×10^{-11} M
D2$_t$	1.66×10^{-10} M	[Gal4p]$_t$	5.47×10^{-9} M
[Gal80p]$_{max}$	1.0×10^{-6} M	[Gal3p]$_{max}$	5.0×10^{-6} M
[Gal$_{int}$]$_{max}$	8×10^{-7} M		

$$\frac{d[y_{20}]}{dt} = K_p f_{2p} D2_t - \mu y_{20} \quad (A.20)$$

$$\frac{d[y_{21}]}{dt} = K_p y_{20} \frac{Gal_{ext}}{k_i + Gal_{ext}} - \mu y_{21} \quad (A.21)$$

$$\frac{d[y_{22}]}{dt} = k_{me} f_{1p} D1_t - \mu y_{22} \quad (A.22)$$

A.3. Algebraic equations

$$f_{1p} = y_5^{0.5} \quad (A.23)$$

$$f_{2p} = (y_6 + y_7)^{0.5} \quad (A.24)$$

$$k_m = k_{max} \frac{y_{21}}{K_s + y_{21}} \quad (A.25)$$

As the glucose and galactose concentrations were fixed during the course of the batch, variables Glu$_{ext}$ and Gal$_{ext}$ assume constant values during a specific batch experiment. The above set of 21 ODEs together with three algebraic equations represents the complete dynamic model for *GAL* regulatory network. These equations were then normalized using suitable normalization constants (Table 1).

The various parameters of the complete dynamic model used in the simulations are tabulated below (see Table 2).

References

[1] Lohr, D., Venkov, P. and Zlatanova, J. (1995) FASEB J. 9, 777–786.
[2] Goldberger, R.F. (1974) Science 183, 810–816.
[3] Savageau, M.A. (1975) Nature 258, 208–214.
[4] Peng, G. and Hopper, J.E. (2000) Mol. Cell. Biol. 20, 5240–5248.
[5] Melcher, K. and Xu, H.E. (2001) EMBO J. 20 (4), 841–851.
[6] Chung, J.D. and Stephanopoulous, G. (1996) Chem. Eng. Sci. 51, 1509–1521.
[7] Ackers, G.K., Johnson, A.D. and Shea, M.A. (1982) Proc. Natl. Acad. Sci. USA 79, 1129–1133.
[8] Santillan, M. and Mackey, M.C. (2001) Proc. Natl. Acad. Sci. USA 98, 1364–1369.
[9] Verma, M., Bhat, P.J. and Venkatesh, K.V. (2003) J. Biol. Chem. 278, 48764–48769.
[10] Venkatesh, K.V., Bhartiya, S. and Ruhela, A. (2004) FEBS Lett. 563, 234–240.
[11] Broach, A.R. (1979) J. Mol. Biol. 131, 41–53.
[12] Johnston, M. and Carlson, M. (1992) in: The Molecular and Cellular Biology of the yeast *Saccharomyces* (Johnes, E.W., Pringle, J.R. and Broach, J.R., Eds.), Cold Spring Harbor Laboratory Press, Plainveiw, New York.
[13] Platt, A. and Reece, R.J. (1998) EMBO J. 17, 4086–4091.
[14] Bhat, P.J. and Murthy, T.V.S. (2001) Mol. Biol. 40 (5), 1066–1069.
[15] Peng, G. and Hopper, J.E. (2002) Proc. Natl. Acad. Sci. USA 99, 8548–8553.
[16] Nehlin, J.O., Carlberg, M. and Ronne, H. (1991) EMBO J. 11, 3373–3377.
[17] Klein, C.J.L., Olsson, L. and Nielsen, J. (1998) Microbiology 144, 13–24.
[18] Griggs, D.W. and Johnston, M. (1991) Proc. Natl. Acad. Sci. USA 88, 8597–8601.
[19] Ren, B., Robert, F., Wyrick, J.J., Aparicio, O., Jennings, E.G., Simon, I., Zeitlinger, J., Schreiber, J., Hannet, N., Kanin, E., Volkert, T.L., Wilson, C.J., Bell, S.P. and Young, R.A. (2000) Science 290, 2306–2309.
[20] Ideker, T., Thorsson, V., Ranish, J.A., Christmas, R., Buhler, J., Eng, J.K., Bumgarner, R., Goodlett, D.R., Aebersold, R. and Hood, L. (2001) Science 292, 929–934.
[21] Fell, D.A. (2001) Trends Genet. 17, 680–682.
[22] Verma, M., Bhat, P.J. and Venkatesh, K.V. (2004) Biotechnol. Appl. Biochem. 39, 89–97.
[23] Blank, T.E., Woods, M.P., Lebo, C.M., Xin, P. and Hopper, J.E. (1997) Mol. Cell. Biol. 17, 2566–2575.
[24] Post-Beittenmiller, M.A., Hamilton, R.W. and Hopper, J.E. (1984) Mol. Cell. Biol. 4, 1235–1245.
[25] Wolfe, K.H. and Shields, D.C. (1997) Nature 387, 708–713.
[26] Kitano, H. (2001) Foundation of System Biology. MIT Press, Cambridge, MA.
[27] Morohashi, M., Winn, A.E., Borisuk, M.T., Bolouri, H., Doyle, J. and Kitano, H. (2002) J. Theor. Biol. 216, 19–30.